Interfacial Polymerization with Electrosprayed Micro-droplets: Towards Controllable and Ultrathin Polyamide Membranes

Xiao-Hua Ma [†, ‡], Zhe Yang [‡], Zhi-Kan Yao [‡], Hao Guo [‡], Zhen-Liang Xu [†], Chuyang Y. Tang [*, ‡]

[†] Shanghai Key Laboratory of Multiphase Materials Chemical Engineering, School of Chemical Engineering, East China University of Science and Technology, 130 Meilong Road, Shanghai 200237, China

[‡] Department of Civil Engineering, The University of Hong Kong, Pokfulam HW619B, Hong Kong, China

[*] To whom all correspondence should be addressed.
Email: tangc@hku.hk; phone: +852 2859 1976; fax: +852 2559 5337.

ABSTRACT: Commercial polyamide membranes for seawater desalination and water purification have low water permeability due to their relatively thick rejection layers. We report a novel interfacial polymerization method to synthesize ultrathin polyamide layers of precisely controllable thickness. Monomer solutions of *m*-phenylenediamine and trimesoyl chloride were electrosprayed into fine micro-droplets. The polymerization reaction between micro-droplets of different monomers leads to a fine and controllable amount of deposition. We fabricated smooth polyamide layers of 4 to several tens of nm in thickness, with growth rate of approximately 1 nm/min. Our study provides a new dimension for the rational design and preparation of ultrathin polyamide membranes with tunable separation properties.

INTRODUCTION

Membrane separation, widely used in seawater desalination and water purification [1], plays a critical role to relieve global water crisis [2]. Among the membranes used for desalination, polyamide membranes are the most commonly used type, thanks to their high permeability, high salt rejection, excellent thermal and mechanical properties [3-4]. Polyamide membranes are typically fabricated by interfacial polymerization of an amine monomer (e.g., *m*-phenylenediamine, MPD) and an acyl chloride monomer (e.g., trimesoyl chloride, TMC) at the interface of an aqueous solution and an organic solution (**Figure 1a**). Their separation performance can be further enhanced by a variety of nanomaterials (e.g., silica [5-6], zeolite [7], graphene oxide [8-11]), water channel proteins [12-13], or metal-organic frameworks [14-16].

In the quest to synthesize membranes with unprecedented permeability, Livingston and coworkers [17] prepared a sub-10 nm polyamide film on a sacrificial layer of cadmium hydroxide nanorods. After removal of the sacrificial layer, this ultrathin polyamide rejection layer showed a greatly improved permeance in comparison with conventional polyamide membranes of typically a few hundred nanometers in thickness [18]. Alternatively, ultrathin polyamide membranes can be prepared via molecular layer-by-layer deposition [19-20]. However, these existing methods involve complex and/or time consuming fabrication steps, which prevent their commercial scaling up.

Here we report fabrication of ultrathin polyamide membranes of a few nanometers to a few tens of nanometers in thickness using a novel interfacial polymerization by electrospray. Electrospray allows us to deliver MPD and TMC solutions in fine micro-droplets of < 1 μL [21] (Figure S1) with desirable amounts to precisely control the thickness of the polyamide rejection layer. A multi-nozzle sprayer with repeated scan enables uniform deposition.

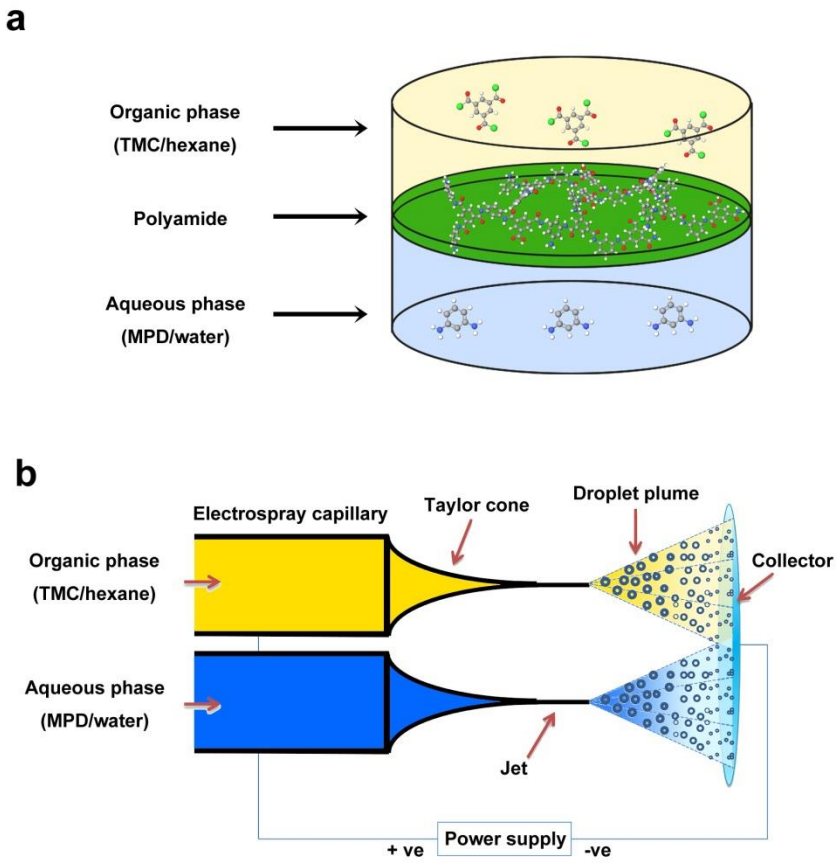

Figure 1. Schematic diagrams of polyamide membrane fabrication process. (a) Schematic of conventional interfacial polymerization reaction. Polymerization reaction takes place at the interface of two immiscible solutions [22]. (b) Schematic of electrospray process. Liquid solution containing functional monomers is introduced into metallic capillary continuously. A very high voltage (e.g., 10-25 kV) is applied to the metallic capillary to charge the solution. The highly charged solution repel with each other due to the same charge. When the solution reaching the capillary tip, it forms a cone shape (known as Taylor cone), which emits a liquid jet through its tip before the droplets burst away from each other into a fine spray. As solvent within these droplets gradually evaporates, forcing the charges within these droplets closer together until the Rayleigh limit is reached and the droplet undergoes Coulomb fission into smaller droplets. The monomers are sprayed onto a substrate that is fixed on a rotating collector. The reaction between the micro-droplets containing MPD and TMC results in the deposition of polyamide material on the collector.

The critical feature to realize interfacial polymerization with electrospray is that two immiscible monomer solutions in micro-droplets encounter on a collector under a strong electrical field (**Figure 1b**). The

reaction among the micro-droplets leads to a fine and controllable amount of deposition each time. We conducted electrospray using traditional monomers, MPD and TMC, which are highly reactive and commonly used in conventional interfacial polymerization. Interfacial polymerization takes place among the micro-droplets containing MPD and TMC monomers to form a polyamide film. The morphologies and properties of the formed polyamide membranes were investigated by scanning electron microscopy (SEM), transmission electron microscopy (TEM), atomic force microscopy (AFM), and filtration tests. Our study provides a new dimension for the preparation ultrathin polyamide membranes with tunable separation properties.

MATERIALS AND METHODS

General Chemicals. A commercial polyether sulfone (PES) ultrafiltration membrane with molecular weight cut-off of 20,000 was purchased from Synder® Filtration and used as substrate. The PES membrane was soaked in de-ionized water overnight before use. TMC (98%), MPD (99%, flakes), hexane, sodium chloride, sodium sulfate and methyl blue were purchased from Sigma-Aldrich and used without further purification.

Fabrication of polyamide membranes. MPD flakes were dissolved in Milli-Q water (Millipore, Billerica, MA) to prepare 2.0 wt.% aqueous solution. TMC was dissolved in hexane to prepare 0.2 wt.% organic solution. To conduct the electrospray experiments, we modified a conventional electrospinning setup (SS-3556H, Ucalery, China) into a multi-nozzle system (Figure 1b). This multi-nozzle system had 6 glass syringes (3 syringes for each monomer solution) that were arranged in an alternative manner at an inter-syringe spacing of 3.2 cm (Figure S2). A stepping motor was used to control their translational movement (100 mm/min over a width of 150 mm) to ensure uniform spray of the monomer solutions onto the

receiving substrate. PES membrane was mounted on a rotating drum (diameter of 10.0 cm) to collect the electrosprayed micro-droplets. Excess amount of water on the PES surface was wiped away with dust-free paper while the interior of the membrane was kept wet. During electrospray, the rotating speed of the drum was 100 rpm. The injection rate of the solution was 1.2 mL/h for each syringe. The distance between the syringe needle tip and the collector was 6.0 cm. The voltage was 13.0 kV, + 10.0 kV for the syringe and - 3.0 kV for the collector. The obtained polyamide membranes with different electrospray time were stored in deionized water overnight before further test.

For comparison, a polyamide thin film composite (TFC) membrane was fabricated by conventional interfacial polymerization method. A 2.0 wt.% MPD aqueous solution was poured onto the PES substrate. After soaking for 2 min, the excess MPD solution was carefully removed by a rubber roller. A 0.2 wt.% TMC hexane solution was then gently poured onto the MPD-soaked PES substrate and the reaction was continued for 2 min. After the reaction, the membrane was cleaned with hexane and soaked in warm deionized water at 50 °C for 10 min. Finally, the polyamide TFC membrane was stored in deionized water at room temperature before further use.

Characterization of polyamide membranes. SEM (Hitachi S4800 FEG SEM) was used to investigate the morphology of the polyamide membranes. Samples were sputtered with gold of approximately 7 nm before characterization. AFM (Veeco NanoScope AFM) was used to measure the surface roughness at a scan rate of 0.6 Hz (5.0 μm ×5.0 μm). The AFM images were analyzed using Gwyddion software. TEM (Philips CM100 TEM) was used to characterize the cross-section of the polyamide membranes. A membrane coupon was embedded in LR white resin [23] and sectioned by an ultramicrotome equipped with a diamond knife. The samples were mounted onto carbon-coated TEM grids for imaging. FTIR was tested by horizontal attenuated

96 total reflectance (HATR, Nicolet 5700, hermo Electron Corp., USA) in the wavenumber range of 4000-400
97 cm^{-1}. Each spectrum was the average of thirty-two scans at a resolution of 4 cm^{-1}. Zeta potential was
98 measured by Electrokinetic Analyzer (Anton Paar® GmbH) using 1.0 mmol/L KCl solution. Contact angle was
99 measured using Attension Theta Goniometer (Biolin Scientific) to determine the surface wetting properties of
100 the polyamide membranes.

101 **Performance of polyamide membranes.** The flux and rejection of the polyamide membranes were
102 measured using a cross-flow filtration system. The feed water contained 100 mg/L methyl blue, 1000 mg/L
103 Na_2SO_4 or 1000 mg/L NaCl. The operating pressure was 6.0 bar [24] for dye rejection and 10.0 bar for salt
104 rejection. During the experiment, the feed solution temperature was controlled at 24 ± 0.1 °C by a circulating
105 chiller. Samples were taken after water flux reached a steady state (approximately 2 hours). The permeation
106 flux was calculated as follows:

107 $$J_w = \frac{\Delta V}{A_m \times \Delta t} \quad (1)$$

108 where J_w represents water flux (L/m^2·h), ΔV represents the volume of the permeate water (L), A_m is the
109 effective area of membrane (42.0 cm^2), and Δt is the duration of permeation (h).

110 The rejection was calculated by:

111 $$R = \left(1 - \frac{C_p}{C_f}\right) \times 100\% \quad (2)$$

112 where C_p and C_f are the permeate concentration and the feed concentration, respectively. Methyl blue
113 concentration was determined by a UV-Vis spectrophotometer (UH-5300, Hitachi Global) at a wavelength of

595 nm. Salt rejection was calculated on the basis of electrical conductivity (Myron L Company, Carlsbad, CA) of the permeate water and the feed water.

$$A = \frac{J_w}{\Delta P - \Delta \pi} \tag{3}$$

where A is the water permeability coefficient, ΔP is the applied pressure and $\Delta \pi$ is the osmotic pressure.

$$R = \frac{J_w}{J_w + B} \tag{4}$$

where B is the solute permeability coefficient.

RESULTS AND DISCUSSION

Membrane Characterization. Polyamide membranes were successfully obtained using 2.0 wt.% MPD aqueous solution and 0.2 wt.% TMC organic solution. These membranes had a smooth surface with a very low average roughness (Ra) of 1.2±0.2 nm (**Figure 2a,b**). For comparison, the TFC membrane fabricated by the conventional interfacial polymerization method using the same monomer concentrations had a ridge-and-valley surface structure with an Ra of 58±2 nm (**Figure 2c,d**). Such roughness structure is typical for conventional polyamide membranes [25] as a result of the rapid and uncontrolled reaction at the interface of two bulk solutions [26-27]. In contrast, liquid solutions were dispersed into micro-droplets (Figure S1) under the electrical field during electrospray [21]. The polymerization reaction between MPD and TMC is confined to the interface of the micro-droplets. Compared to conventional bulk interfacial polymerization, the electrospray system provides a more stable interface for the reaction thanks to the greater interfacial tension of the micro-droplets [28]. The drop-wise deposition forms a smooth polyamide film, which is essential for further

controlling the film thickness. In addition, smoother membrane surface is known to have better antifouling performance [29].

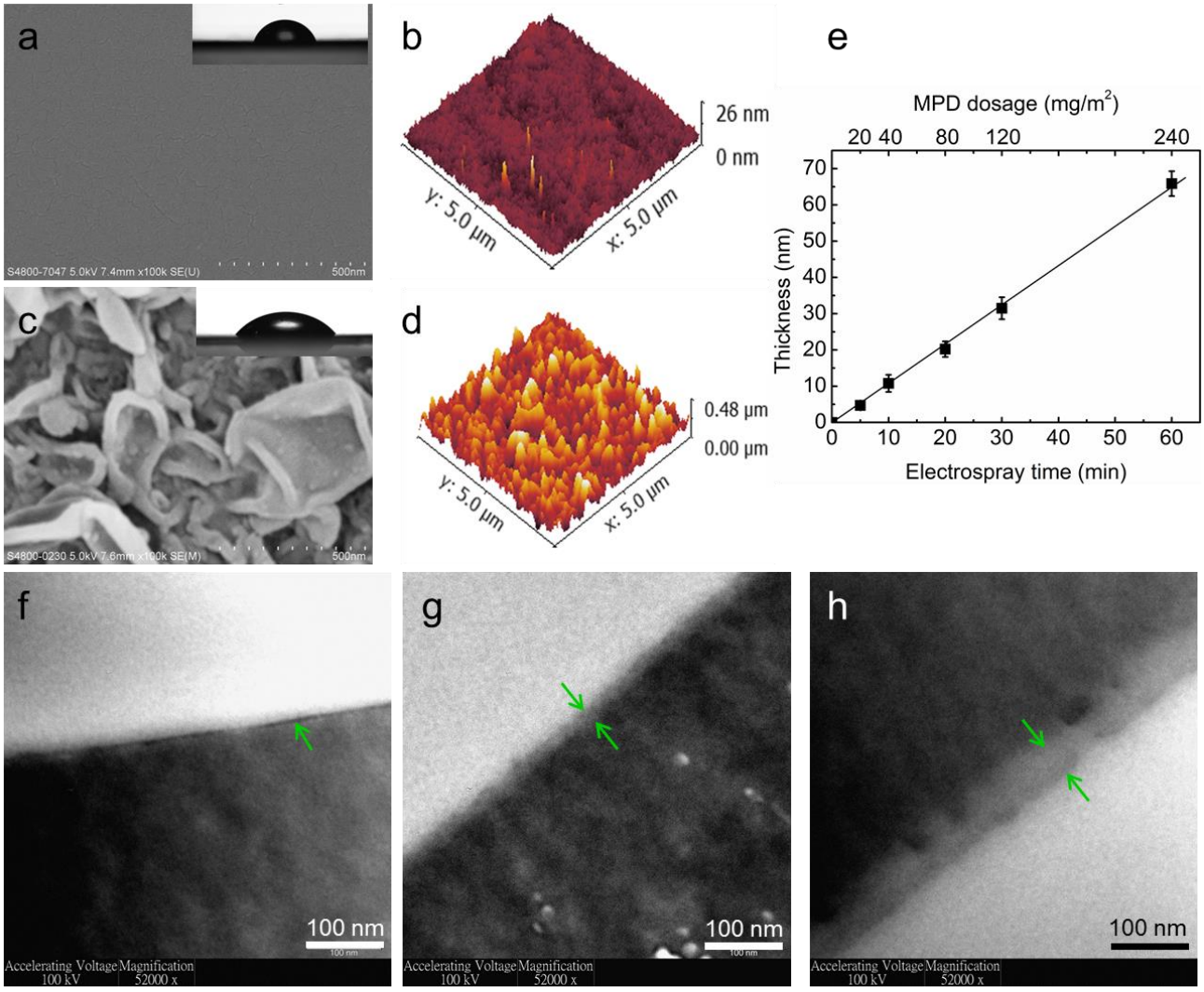

Figure 2. Morphologies and thickness of polyamide membranes. SEM (a) and AFM (b) images of polyamide membrane fabricated by electrospray of 20 min. SEM (c) and AFM (d) images of TFC polyamide membrane fabricated by conventional interfacial polymerization. The thickness of polyamide film grew linearly as electrospray time increased (e). TEM cross-sectional images of polyamide membranes fabricated at 5 min (f), 30 min (g) and 60 min (h). All these polyamide membranes were fabricated by using 2.0 wt.% MPD aqueous solution and 0.2 wt.% TMC hexane organic solution. The error bars in part (e) were the standard deviation based on at least three replicate samples.

The thickness of the polyamide thin-film layer was only 4 nm at 5 min and grew linearly at

approximately 1 nm/min as electrospray time increased (**Figure 2e-h**). This result demonstrates that the thickness of the polyamide rejection layer can be finely controlled. In addition, the rate of polyamide film growth can be potentially controlled by adjusting the monomer dosage (i.e., the number of nozzles × volumetric rate of spray per nozzle × monomer concentration). TEM (**Figure 2f-h**) and SEM (Figure S3) shows that the rejection layer was uniform with a smooth surface.

Water contact angle of electrospray fabricated polyamide membrane was 72.0±2.1 ° (**Figure 2a**), while that of the conventional TFC membrane was 53.3±2.9 ° (**Figure 2c**). This difference in apparent contact angles (measured values) can be attributed to the change in surface roughness. After correction for roughness effect using Wenzel equation [30], the conventional TFC membrane had an intrinsic contact angle of 71.3 °, nearly identical to the electrosprayed polyamide membrane.

FTIR measurements show identical characteristic peaks of both polyamide membranes (Figure S5a). Peaks at 1630 cm^{-1} and 1520 cm^{-1} correspond to N−C=O and C−N−H vibrations, respectively [31-32], both of which can be assigned to the amide linkages in the polyamide layer. However, the electrosprayed polyamide membrane had much weaker peak intensities due to its much thinner layer. The two membranes had nearly identical zeta potential values over pH 3-9, and both membranes had isoelectric point at pH 3.7 (Figure S5b).

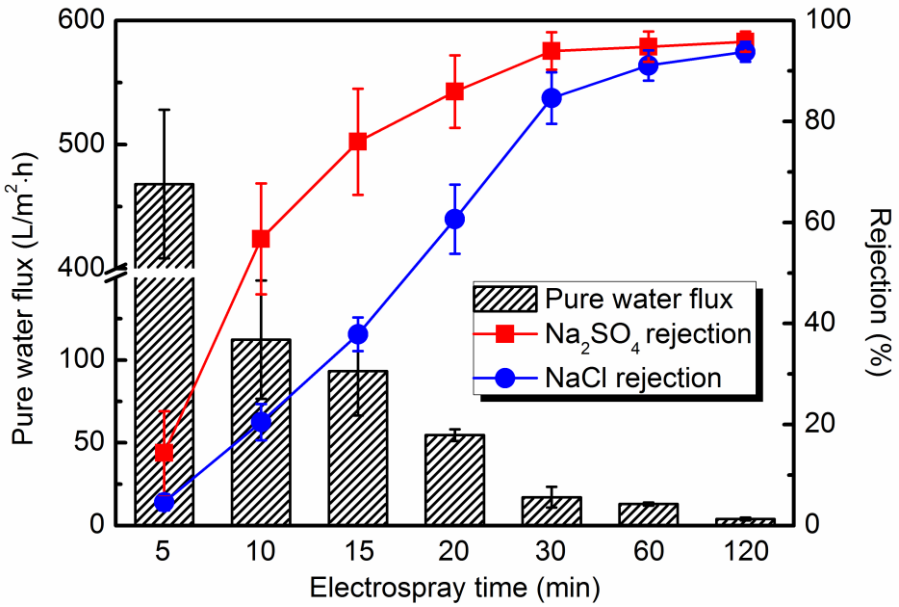

158

159 **Figure 3.** Separation performances of polyamide membranes fabricated at different electrospray time. All these polyamide
160 membranes were fabricated by using 2.0 wt.% MPD aqueous solution and 0.2 wt.% TMC hexane organic solution. For the
161 salt rejection was tested by using a 1000 ppm NaCl or Na_2SO_4 feed solution at 10.0 bar.

162

163 **Separation performance.** We evaluated separation performances of the electrosprayed polyamide
164 membranes via cross-flow filtration. **Figure 3** presents water flux and rejection of these membranes as a
165 function of the electrospray time. At 5 min, the flux could reach 440 L/m^2·h with NaCl rejection of 4.6% and
166 Na_2SO_4 rejection of 14.4%. As electrospray time increased to 30 min, the flux decreased to 17.0 L/m^2·h
167 accompanied with significant increase in salt rejection (NaCl of 84.7% and Na_2SO_4 of 94.0%). The NaCl
168 rejection further reached 93.8% at 120 min. These results show the feasibility of fine-tuning separation
169 properties by adjusting the electrospray time. We further evaluated the rejection performance of these
170 membranes using 100 ppm dye solution (methyl blue, Mw = 799.8). Dye rejection of 91.0% was achieved at
171 10 min, and complete dye rejection occurred at electrospray time of ≥ 20 min. The finely tunable separation
172 properties allow these polyamide membranes to be used in different membrane processes ranging from loose
173 nanofiltration to reverse osmosis.

Figure 4 plots the water-salt permselectivity (A/B_{NaCl}) vs. water permeability (A) of the electrosprayed membranes and the TFC polyamide membrane prepared by conventional interfacial polymerization using identical monomer solutions. For comparison, the water permeability and NaCl rejection of commercial polyamide membranes (BW30 and SW30) are also shown. Electrosprayed membranes (e.g., at 60 min) had better water permeability and selectivity compared with the conventional TFC membrane. Nevertheless, its performance was not as good as the commercial BW30 and SW30. It is worthwhile to note that the commercial recipes of polyamide membranes have been highly optimized in terms of monomer concentrations and additives used for interfacial polymerization. A critical aspect to be further addressed is to enhance salt rejection by improving the uniformity of the rejection layers and hence minimizing defects in electrosprayed membranes. In the current study, we show the feasibility of further increasing salt rejection by using greater monomer concentrations (Figure S7,8), increased spray rate (Figure S9) and the addition of a surfactant sodium dodecyl sulfate to the MPD aqueous solution (Figure S4). Alternatively, the properties of the fabricated polyamide membrane can be further tuned through controlling the surface pore size of the substrate [33], changing monomer chemistry and incorporating functional nanomaterials [34]. Future studies shall further investigate additional factors such as the size of the micro-droplets and the rate of evaporation of solvents.

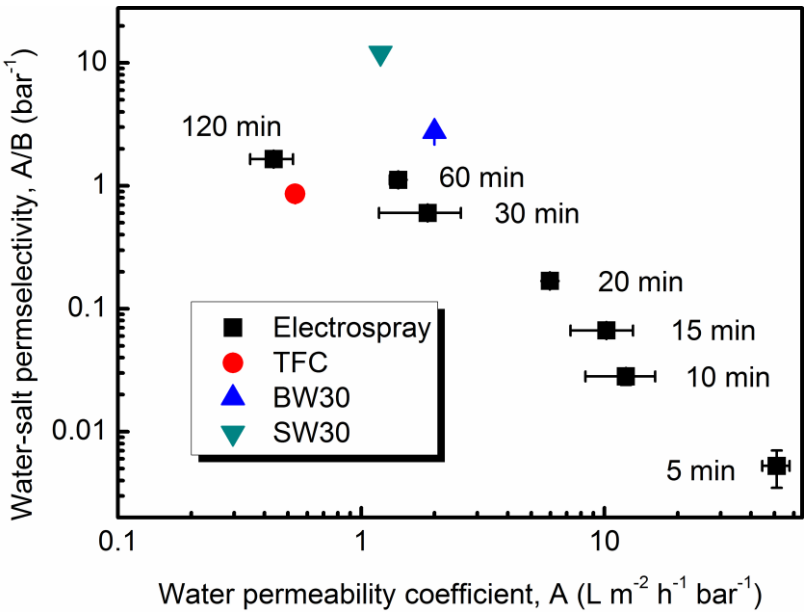

Figure 4. Water-salt permselectivity (A/B_{NaCl}) vs. water permeability (A) of electrosprayed membranes, a conventional TFC membrane, and commercial polyamide membranes BW30 and SW30. A is the water permeability coefficient and B_{NaCl} is the NaCl permeability coefficient. The electrosprayed membranes and the conventional TFC membrane were prepared using identical monomer solutions (2.0 wt.% MPD aqueous solution and 0.2 wt.% TMC hexane organic solution).

In the current study, we show for the first time to fabricate polyamide membranes via electrospray-assisted interfacial polymerization, which enables monomers to react at the interface of fine micro-droplets. In contrast, conventional interfacial polymerization taken place at the interface between two bulk liquids is more susceptible to disturbance (e.g., heat released from the interfacial polymerization [17]) and is known to form a rough membrane surface. In our work, the improved dispersion of the monomers and the more stable reaction interface during electrospray-assisted interfacial polymerization enable the creation of ultrathin polyamide rejection layer with minimal surface roughness. The fine addition of polyamide by electrospray resulted in rejection layers ranging from sub-10 nm to a few tens of nm, which can be controlled by the electrospray time. The method allows monomers to be used more effectively with less wastage, which allows a greener production. The reduced wastage can also provide a critical advantage in cases where

expensive chemicals are to be used. The method can be potentially scaled up by the inclusion of well-designed arrays of hundreds of nozzles to reduce the spray time and to improve membrane uniformity, much like the commercial production of electrospun nanofibrous membranes [35]. The versatility of this electrospray approach potentially offers a new pathway to the design of a wide variety of membranes and films applicable to surface coatings, gas separation membranes, microfluidics, sensors, and bio-devices.

ASSOCIATED CONTENT

Supporting Information

The Supporting Information is available free of charge on the ACS Publications website. S1. Characterization of electrosprayed micro-droplets; S2. Schematic diagram of syringe array used for electrospray; S3. Effect of surfactant addition on membrane surface morphology and separation performance; S4. FTIR and zeta potential characterization; S5. Separation performance of electrosprayed polyamide membrane over an 18-hour filtration test; S6. Effect of monomer concentration and spray rate on membrane separation performance.

AUTHOR INFORMATION

Corresponding author

* Email: tangc@hku.hk. Phone: +852 28591976.

Notes

The authors declare no competing financial interests.

ACKNOWLEDGMENTS

The authors gratefully acknowledge the research funding provided by Hong Kong Scholars Program (No. XJ2015015), General Research Fund (Project 17207514) of the Research Grants Council of Hong Kong, the Strategic Research Theme (Clean Energy) at the University of Hong Kong, National Natural Science Foundation of China (21406060), Fundamental Research Funds for the Central Universities (WA1514305) and China Postdoctoral Science Foundation (2016M601527).

REFERENCES

1. Li, D.; Wang, H. T., Recent developments in reverse osmosis desalination membranes. *Journal of Materials Chemistry* **2010,** *20*, 4551-4566.
2. Elimelech, M.; Phillip, W. A., The Future of Seawater Desalination: Energy, Technology, and the Environment. *Science* **2011,** *333*, 712-717.
3. Lee, K. P.; Arnot, T. C.; Mattia, D., A review of reverse osmosis membrane materials for desalination-Development to date and future potential. *Journal of Membrane Science* **2011,** *370* , 1-22.
4. Lau, W. J.; Ismail, A. F.; Misdan, N.; Kassim, M. A., A recent progress in thin film composite membrane: A review. *Desalination* **2012,** *287*, 190-199.
5. Baig, M. I.; Ingole, P. G.; Choi, W. K.; Jeon, J. D.; Jang, B.; Moon, J. H.; Lee, H. K., Synthesis and characterization of thin film nanocomposite membranes incorporated with surface functionalized Silicon nanoparticles for improved water vapor permeation performance. *Chemical Engineering Journal* **2017,** *308*, 27-39.
6. Tian, M.; Wang, Y. N.; Wang, R.; Fane, A. G., Synthesis and characterization of thin film nanocomposite forward osmosis membranes supported by silica nanoparticle incorporated nanofibrous substrate. *Desalination* **2017,** *401*, 142-150.
7. Pendergast, M. M.; Hoek, E. M. V., A review of water treatment membrane nanotechnologies. *Energ Environ Sci* **2011,** *4*, 1946-1971.
8. Hu, M.; Zheng, S. X.; Mi, B. X., Organic Fouling of Graphene Oxide Membranes and Its Implications for Membrane Fouling Control in Engineered Osmosis. *Environmental science & technology* **2016,** *50* , 685-693.
9. Hegab, H. M.; Zou, L. D., Graphene oxide-assisted membranes: Fabrication and potential applications in desalination and water purification. *Journal of Membrane Science* **2015,** *484*, 95-106.
10. Perreault, F.; Tousley, M. E.; Elimelech, M., Thin-Film Composite Polyamide Membranes Functionalized with Biocidal Graphene Oxide Nanosheets. *Environ Sci Tech Let* **2014,** *1*, 71-76.
11. Mi, B. X., Graphene Oxide Membranes for Ionic and Molecular Sieving. *Science* **2014,** *343*, 740-742.
12. Tang, C. Y.; Wang, Z. N.; Petrinic, I.; Fane, A. G.; Helix-Nielsen, C., Biomimetic aquaporin membranes coming of

age. *Desalination* **2015,** *368*, 89-105.
13. Kumar, M.; Grzelakowski, M.; Zilles, J.; Clark, M.; Meier, W., Highly permeable polymeric membranes based on the incorporation of the functional water channel protein Aquaporin Z. *P Natl Acad Sci USA* **2007,** *104*, 20719-20724.
14. Liu, X. L.; Demir, N. K.; Wu, Z. T.; Li, K., Highly Water-Stable Zirconium Metal Organic Framework UiO-66 Membranes Supported on Alumina Hollow Fibers for Desalination. *Journal of the American Chemical Society* **2015,** *137*, 6999-7002.
15. Sorribas, S.; Gorgojo, P.; Tellez, C.; Coronas, J.; Livingston, A. G., High Flux Thin Film Nanocomposite Membranes Based on Metal-Organic Frameworks for Organic Solvent Nanofiltration. *Journal of the American Chemical Society* **2013,** *135*, 15201-15208.
16. Wang, C. H.; Liu, X. L.; Demir, N. K.; Chen, J. P.; Li, K., Applications of water stable metal-organic frameworks. *Chemical Society Reviews* **2016,** *45*, 5107-5134.
17. Karan, S.; Jiang, Z.; Livingston, A. G., Sub–10 nm polyamide nanofilms with ultrafast solvent transport for molecular separation. *Science* **2015,** *348*, 1347-1351.
18. Klosowski, M. M.; McGilvery, C. M.; Li, Y. Q.; Abellan, P.; Ramasse, Q.; Cabral, J. T.; Livingston, A. G.; Porter, A. E., Micro-to nano-scale characterisation of polyamide structures of the SW30HR RO membrane using advanced electron microscopy and stain tracers. *Journal of Membrane Science* **2016,** *520*, 465-476.
19. Gu, J. E.; Lee, S.; Stafford, C. M.; Lee, J. S.; Choi, W.; Kim, B. Y.; Baek, K. Y.; Chan, E. P.; Chung, J. Y.; Bang, J.; Lee, J. H., Molecular Layer-by-Layer Assembled Thin-Film Composite Membranes for Water Desalination. *Advanced Materials* **2013,** *25*, 4778-4782.
20. Song, X.; Qi, S.; Tang, C. Y.; Gao, C., Ultra-thin, multi-layered polyamide membranes: Synthesis and characterization. *Journal of Membrane Science* **2017,** *540*, 10-18.
21. Girod, M.; Moyano, E.; Campbell, D. I.; Cooks, R. G., Accelerated bimolecular reactions in microdroplets studied by desorption electrospray ionization mass spectrometry. *Chem Sci* **2011,** *2*, 501-510.
22. Raaijmakers, M. J. T.; Benes, N. E., Current trends in interfacial polymerization chemistry. *Progress in Polymer Science* **2016,** *63*, 86-142.
23. Pacheco, F.; Sougrat, R.; Reinhard, M.; Leckie, J. O.; Pinnau, I., 3D visualization of the internal nanostructure of polyamide thin films in RO membranes. *Journal of Membrane Science* **2016,** *501*, 33-44.
24. Lin, J.; Tang, C. Y.; Ye, W.; Sun, S.-P.; Hamdan, S. H.; Volodin, A.; Van Haesendonck, C.; Sotto, A.; Luis, P.; Van der Bruggen, B., Unraveling flux behavior of superhydrophilic loose nanofiltration membranes during textile wastewater treatment. *Journal of Membrane Science* **2015,** *493*, 690-702.
25. Tang, C. Y. Y.; Kwon, Y. N.; Leckie, J. O., Effect of membrane chemistry and coating layer on physiochemical properties of thin film composite polyamide RO and NF membranes II. Membrane physiochemical properties and their dependence on polyamide and coating layers. *Desalination* **2009,** *242*, 168-182.
26. Freger, V., Nanoscale Heterogeneity of Polyamide Membranes Formed by Interfacial Polymerization. *Langmuir* **2003,** *19*, 4791-4797.
27. Ghosh, A. K.; Jeong, B. H.; Huang, X. F.; Hoek, E. M. V., Impacts of reaction and curing conditions on polyamide composite reverse osmosis membrane properties. *Journal of Membrane Science* **2008,** *311*, 34-45.
28. Shen, F.; Li, Y.; Liu, Z.-M.; Cao, R.-T.; Wang, G.-R., Advances in Micro-Droplets Coalescence Using Microfluidics. *Chinese J Anal Chem* **2015,** *43*, 1942-1954.
29. Zhu, X. H.; Elimelech, M., Colloidal fouling of reverse osmosis membranes: Measurements and fouling mechanisms. *Environmental Science and Technology* **1997,** *31*, 3654.
30. Wolansky, G.; Marmur, A., Apparent contact angles on rough surfaces: the Wenzel equation revisited. *Colloid Surface A* **1999,** *156*, 381-388.
31. Xie, W.; Geise, G. M.; Freeman, B. D.; Lee, H.-S.; Byun, G.; McGrath, J. E., Polyamide interfacial composite

299 membranes prepared from m-phenylene diamine, trimesoyl chloride and a new disulfonated diamine. *Journal of*
300 *Membrane Science* **2012,** *403*, 152-161.
301 32. Tang, C. Y.; Kwon, Y.-N.; Leckie, J. O., Effect of membrane chemistry and coating layer on physiochemical
302 properties of thin film composite polyamide RO and NF membranes. *Desalination* **2009,** *242*, 149-167.
303 33. Cheng, Z. L.; Li, X.; Feng, Y. N.; Wan, C. F.; Chung, T. S., Tuning water content in polymer dopes to boost the
304 performance of outer-selective thin-film composite (TFC) hollow fiber membranes for osmotic power generation.
305 *Journal of Membrane Science* **2017,** *524*, 97-107.
306 34. Yang, Z.; Ma, X.-H.; Tang, C. Y., Recent development of novel membranes for desalination. *Desalination*
307 doi.org/10.1016/j.desal.2017.11.046.
308 35. http://inovenso.com/portfolio-view/nanospinner416/.

309

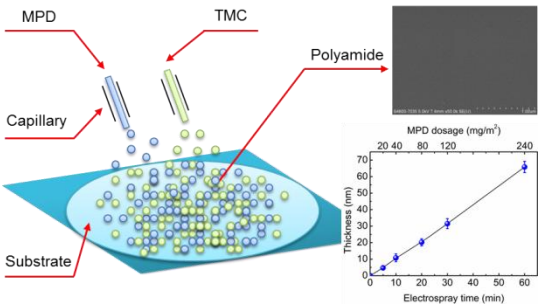

310

311

312

Supporting Information

Interfacial Polymerization with Electrosprayed Micro-droplets: Towards Controllable and Ultrathin Polyamide Membranes

Xiao-Hua Ma [†, ‡], Zhe Yang [‡], Zhi-Kan Yao [‡], Hao Guo [‡], Zhen-Liang Xu [†], Chuyang Y. Tang [*, ‡]

[†] Shanghai Key Laboratory of Multiphase Materials Chemical Engineering, School of Chemical Engineering, East China University of Science and Technology, 130 Meilong Road, Shanghai 200237, China

[‡] Department of Civil Engineering, The University of Hong Kong, Pokfulam HW619B, Hong Kong, China

Email: * tangc@hku.hk; phone: +852 2859 1976; fax: +852 2559 5337.

Number of pages (including the cover page): 10

Number of figures: 9

Number of tables: 0

S1. Characterization of electrosprayed micro-droplets

Due to the small size of the electrosprayed micro-droplets and their highspeed movement in the electrical field, it is difficult to directly measure their exact dimension. In this study, we used an indirect method to characterize the size of the micro-droplets. Specifically, a dyed solution (100 mg/L methyl blue) was electrosprayed onto a microscope slide and the trace of the dye was imaged by an optical microscope (EVOS® FL Auto Imaging System). The electrospray time was 30 seconds. The results are shown in Figure S1. Based on this method, we can infer that the size of the micro-droplets was on the order of 100 μm. It is worthwhile to note that the height of the collected micro-droplets is expected to be significantly smaller than the lateral dimension due to the flattened shape.

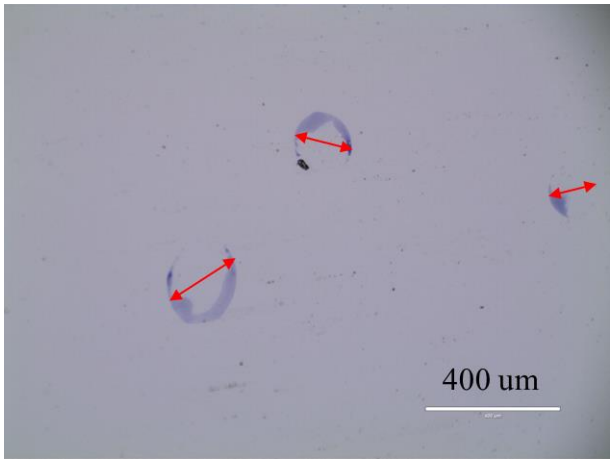

Figure S1. Optical micrograph of micro-droplets of dyed water (methyl blue) collected on a microscope slide. The electrospray time was 30 seconds.

S2. Schematic diagram of syringe array used for electrospray

A schematic diagram of the array of syringes is shown in Figure S2. The array consisted 6 syringes that were arranged at an inter-syringe spacing of 3.2 cm.

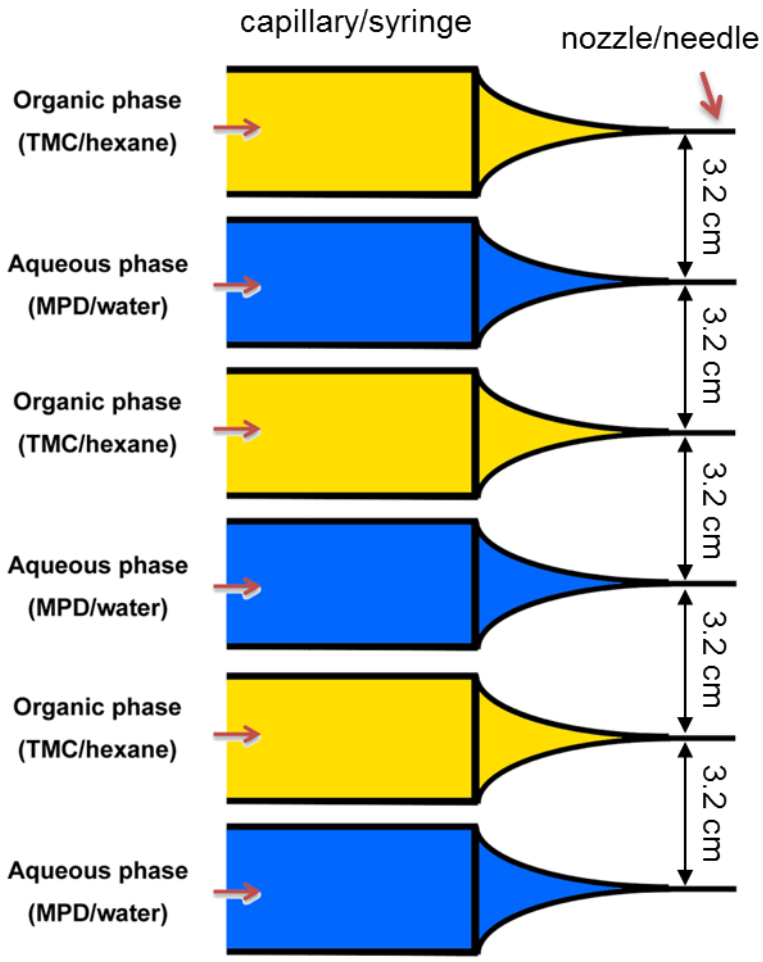

Figure S2. A schematic diagram of the arrangement of 6 syringes and the inter-syringe spacing.

S3. Effect of surfactant addition on membrane surface morphology and separation performance

Figure S3A shows the SEM micrograph of membranes prepared using 2.0 wt.% MPD aqueous solution and 0.2 wt.% TMC hexane organic solution at electrospray time of 5. SEM images show some localized defects at the low electrospray time of 5 min. Longer electrospray time (e.g., 15 min) and/or the including of a surfactant (4.0 mM sodium dodecyl sulfate, SDS) appeared to be effective in minimizing defects formation (Figure S3B,C,D). Figure S4 shows that SDS addition was effective in enhancing the salt rejection of electrosprayed polyamide membranes, which further confirms its ability to prevent defect deformation.

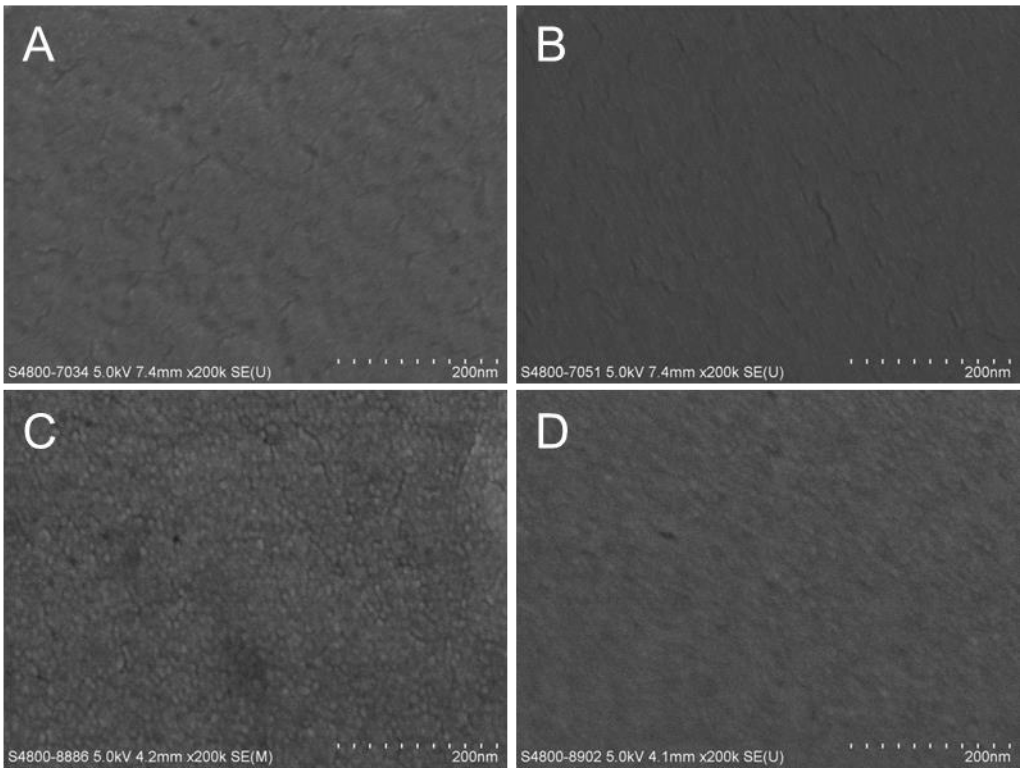

Figure S3. SEM images of polyamide membrane fabricated by electrospray of (A) 5 min, (B) 15 min, (C) 5 min with 4.0 mM SDS surfactant, and (D) 15 min with 4.0 mM SDS surfactant.

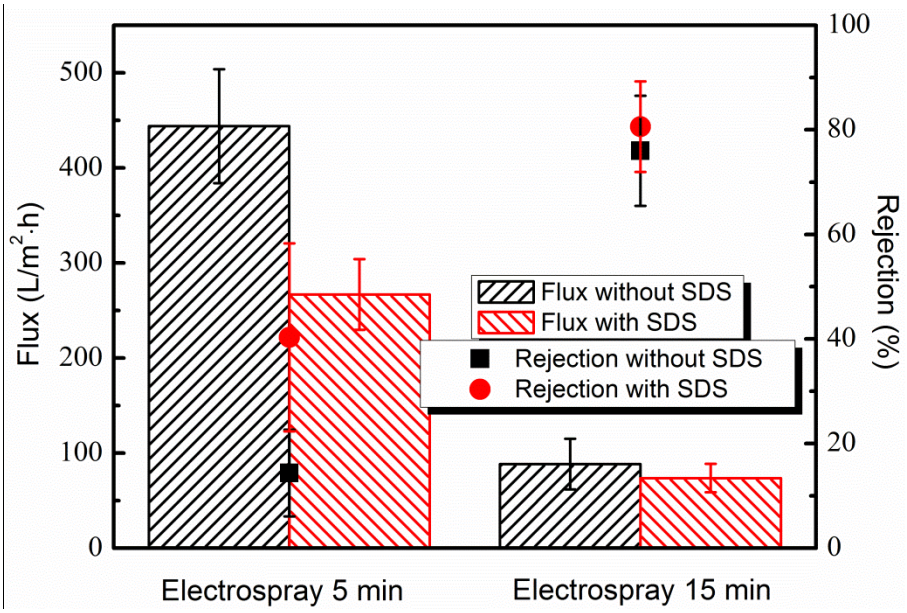

Figure S4. Separation performance (flux and Na_2SO_4 rejection) of polyamide membrane with and without SDS (4 mM) fabricated by electrospray.

S4. FTIR and zeta potential characterization

FTIR spectra (Figure S5a) of the polyamide membranes prepared by electrospray and conventional interfacial polymerization were obtained by horizontal attenuated total reflectance (HATR, Nicolet 5700, hermo Electron Corp., USA). The characteristic peaks of polyamide at 1630 cm^{-1} (N−C=O vibration) and 1520 cm^{-1} (N−C=O vibration) were present for both membranes. The zeta potential curves of the two membranes were nearly identical (Figures S5b).

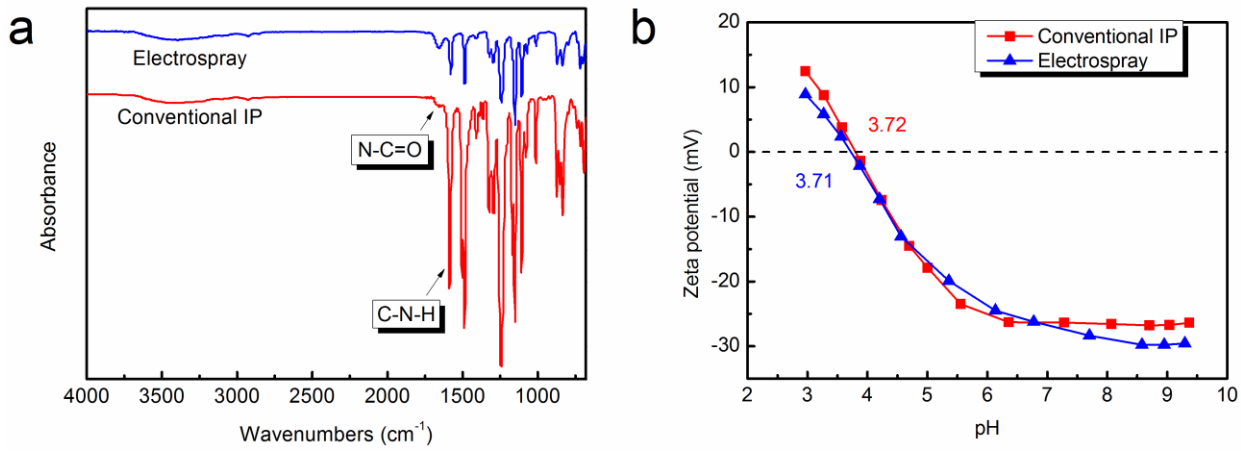

Figure S5. FTIR (a) and zeta potential (b) measurements of polyamide membrane fabricated by conventional interfacial polymerization and electrospray (10 min).

S5. Separation performance of electrosprayed polyamide membrane over an 18-hour filtration test

Figure S6 shows the flux and rejection of the membrane (electrospray time = 5 min) over an 18-hour cross-flow filtration test using a 1000 ppm $NaSO_4$ feed solution. The membrane showed stable rejection during the test. The slight increase in rejection was due to membrane compaction.

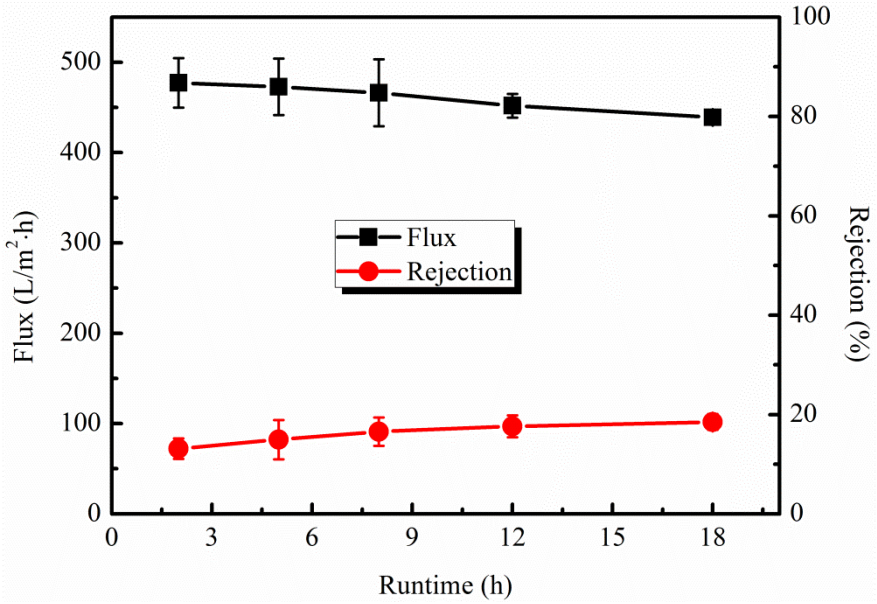

Figure S6. Separation performances (flux and Na_2SO_4 rejection) of polyamide membrane fabricated at 5 min vs. runtime under cross-flow conditions at 10 bar over 18 hours. The feed solution contained 1000 ppm Na_2SO_4.

S6. Effect of monomer concentration and spray rate on membrane separation performance

We have performed additional tests of using higher monomer concentrations and spray rate. Under the same electrospray time, higher monomer concentration enhanced the membrane rejection, particularly at the shorter electrospray time of 5 min (Figure S7). We further conducted tests using membranes with identical loading of monomers (by using different combinations of monomer concentrations and electrospray time, see Figure S8). The membrane prepared by 2.0 wt. % MPD/0.2 wt. % TMC at 10 min and that prepared by 1.0 wt. % MPD/0.1 wt.% TMC at 20 min showed nearly identical rejection, suggesting that the growth of rejection layer is likely controlled by the mass loading of the monomers. Nevertheless, membrane rejection start to be sacrificed when the electrospray time was further reduced to 5 min, which might be caused by a less uniform deposition.

In addition, we fabricated electrosprayed polyamide membranes at different spray rate. The filtration test results were shown in Figure S9. By doubling the spray rate from 1.2 mL/h to 2.4 mL/h at an identical electrospray time of 5 min, Na_2SO_4 rejection was significantly increased at the expense of reduced water flux.

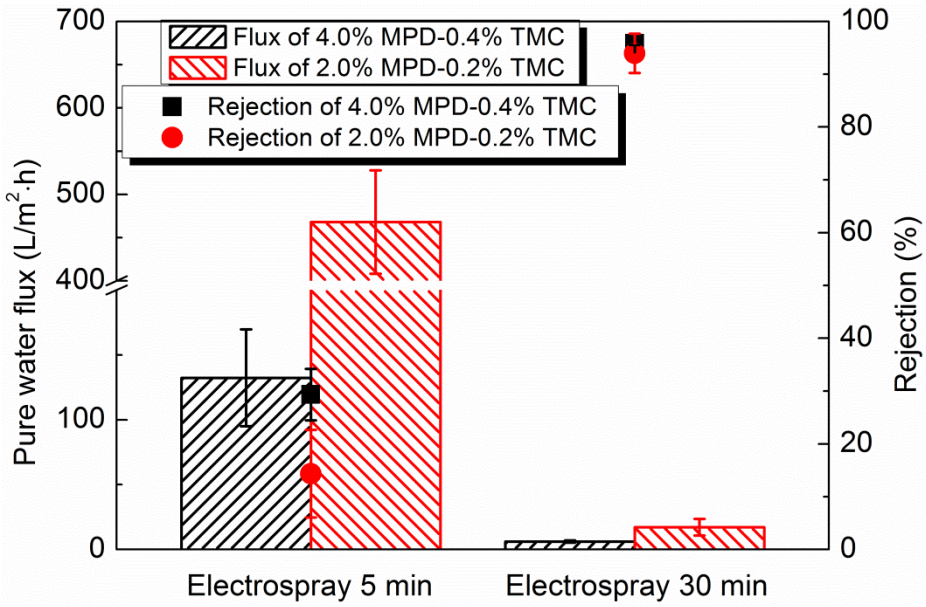

Figure S7. Separation performances (pure water flux and Na_2SO_4 rejection) of polyamide membranes with different monomer concentrations at electrospray time of 5 min and 30 min.

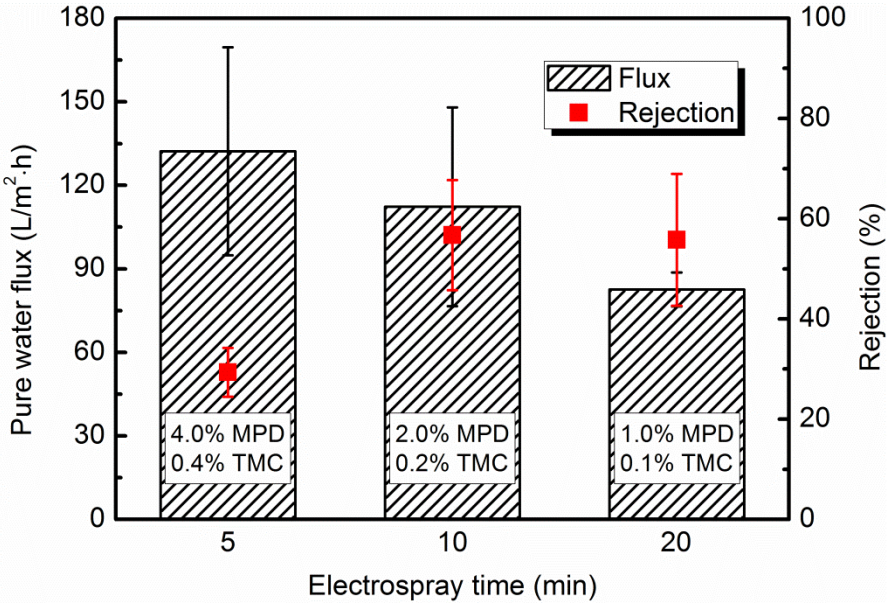

94

95 **Figure S8**. Separation performances (pure water flux and Na_2SO_4 rejection) of polyamide membranes with electrospray of

96 identical monomer loading on the substrate.

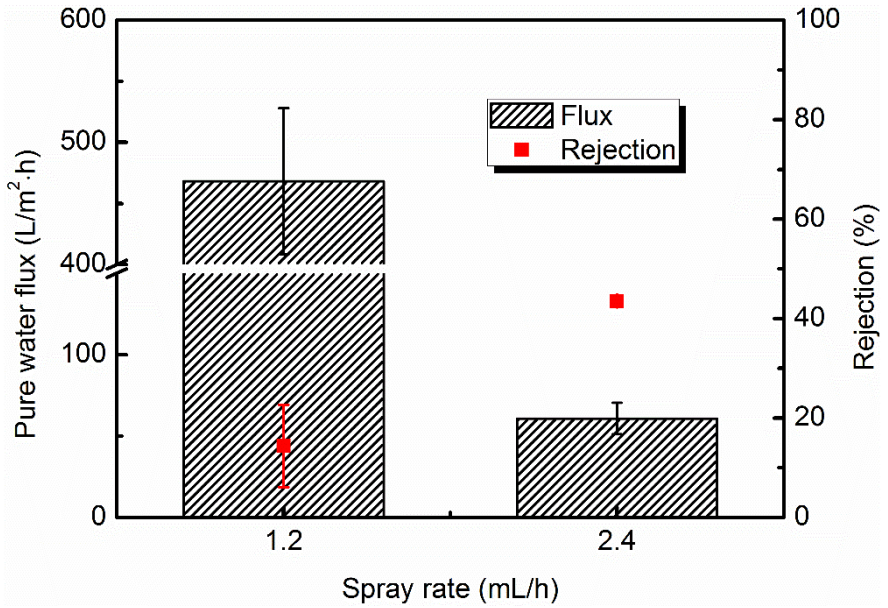

97

98 **Figure S9**. Separation performances (pure water flux and Na_2SO_4 rejection) of polyamide membranes with different spray

99 rate at electrospray time of 5 min.